Bio-Inspired Cryo-Ink Preserves Red Blood Cell Phenotype and Function During Nanoliter Vitrification

*Rami El Assal, Sinan Guven, Umut Atakan Gurkan, Irep Gozen, Hadi Shafiee, Sedef Dalbeyler, Noor Abdalla, Gawain Thomas, Wendy Fuld, Ben M. W. Illigens, Jessica Estanislau, Joseph Khoory, Richard Kaufman, Claudia Zylberberg, Neal Lindeman, Qi Wen, Ionita Ghiran, and Utkan Demirci**

The unique morphology and mechanics of red blood cells (RBCs) are critical in influencing their function.[1] Recent studies have revealed detrimental alterations in RBC morphological, mechanical, and functional properties (collectively termed as "storage injury") during RBC hypothermic liquid preservation.[2] Such adverse storage changes correlate with increased mortality and morbidity rates in medically compromised patients when RBCs are stored for more than 14 days.[3]

Cryopreservation has emerged as an alternative approach that extends the RBC preservation period for years by overcoming the adverse changes that occur in liquid preservation. Although RBC cryopreservation is clinically employed, adverse morphological,[4] mechanical,[5] and functional[6] changes still present challenges. Current RBC cryopreservation techniques utilize glycerol in slow-freezing[7] and rapid-freezing techniques.[5,3,8] Several causative factors have been shown to be involved in cryo-injury; however, cryoprotective agent (CPA) used, as well as cooling and rewarming approaches, are detrimental.[9] In contrast, vitrification, in which cells are transformed into a glassy-state, has emerged as an alternative to the presently applied means of cryopreservation. However, conventional vitrification requires high concentrations of CPAs to achieve successful vitrification. CPA acts as antifreeze to the cytosol and as a stabilizer for the plasma membrane; but, it is toxic to cells when used in high concentrations.[9,10] Although vitrification has shown advantages over traditional cryopreservation techniques, it has not been incorporated into transfusion medicine mainly due to an inability to achieve vitrification with bulk volumes and throughput challenges. Therefore, innovative technologies for vitrification could improve RBC preservation success, which is urgently needed to advance the clinical practice of transfusion medicine and expand RBC preservation options for patients. Moreover, the use of bio-inspired materials in this context can offer additional benefits.[11]

Recent advances in manipulating cells and droplets have been made, particularly at the interface between bioengineering, biomaterials, and medicine.[12] In one important instance, a new technology-enabled capability of printing viable

Dr. R. El Assal, Dr. S. Guven, Dr. U. Demirci
Bio-Acoustic-MEMS in Medicine (BAMM) Laboratory
Canary Center at Stanford for Cancer Early Detection
Department of Radiology
Stanford University School of Medicine
Palo Alto, CA 94304, USA
E-mail: utkan@stanford.edu

Dr. R. El Assal, Dr. S. Guven, Dr. U. A. Gurkan, Dr. I. Gozen, Dr. H. Shafiee, S. Dalbeyler, N. Abdalla, Dr. U. Demirci
Bio-Acoustic-MEMS in Medicine (BAMM) Laboratory
Division for Biomedical Engineering
Division of Infectious Diseases, Renal Division
Department of Medicine, Brigham and Women's Hospital
Harvard Medical School
Cambridge, MA 02139, USA

Dr. U. A. Gurkan
Case Western Reserve University
Biomanufacturing and Microfabrication Laboratory
Mechanical and Aerospace Engineering Department
Department of Orthopedics
Advanced Platform Technology Center
Louis Stokes Cleveland Veterans Affairs Medical Center
Cleveland, OH 44106, USA

G. Thomas, Dr. Q. Wen
Department of Physics
Worcester Polytechnic Institute
Worcester, MA 01609, USA

W. Fuld, Dr. N. Lindeman
Department of Pathology
Brigham and Women's Hospital,
Harvard Medical School
Boston, MA 02115, USA

Dr. B. M. W. Illigens
Department of Neurology
Beth Israel Deaconess Medical Center
Harvard Medical School
Boston, MA 02215, USA

J. Estanislau, J. Khoory, Dr. I. Ghiran
Division of Infectious Disease and Allergy-Inflammation
Department of Medicine
Beth Israel Deaconess Medical Center
Harvard Medical School
Boston, MA 02115, USA

Dr. R. Kaufman
Brigham and Women's Hospital Blood Bank
Division of Adult Transfusion Medicine
Department of Pathology
Brigham and Women's Hospital,
Harvard Medical School
Boston, MA 02115, USA

Dr. C. Zylberberg
Akron Biotechnology, LLC
Boca Raton, FL 33487, USA

DOI: 10.1002/adma.201400941

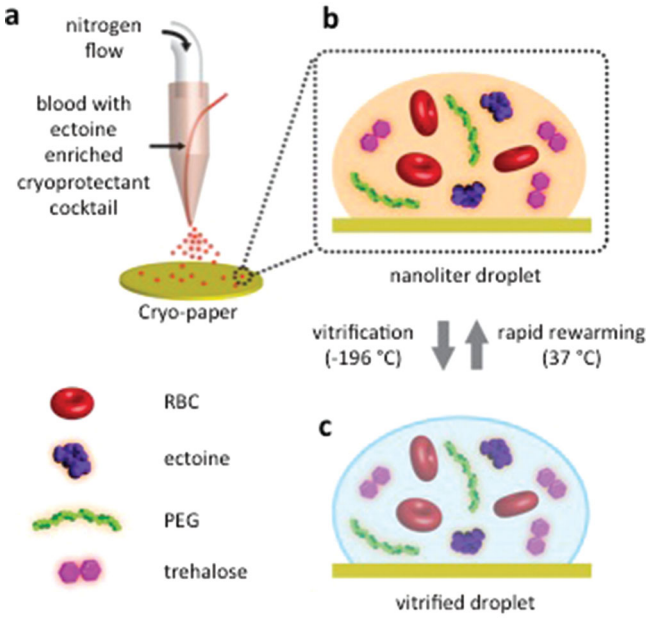

Figure 1. Droplet-based vitrification of red blood cells. a) The essentials of the experimental setup for the droplet formation. The system consists of nitrogen gas flow and a droplet deposition system controlled by a syringe pump. The droplets are generated from the co-flow stream of cryoprotective agent (CPA)-loaded red blood cell (RBC) mixture as the nitrogen gas flows through a droplet ejector, which transforms the bulk of the sample into nanoliter droplets. The CPA consists of a cocktail solution of ectoine, trehalose, and polyethylene glycol (PEG). The droplets were ejected on a cryo-paper (polyethylene collection film). b) Schematic magnified view of a single droplet on the cryo-paper including RBCs, ectoine, trehalose, and PEG. c) Schematic view of the vitrified droplet in (b). Vitrification is achieved by submersing the cryo-paper into liquid nitrogen. The vitrified droplet transforms to (b) after rapid thawing of the cells on a cryo-paper in phosphate-buffered saline at 37 °C.

and functional cells has been reported.[51,13] In the present study, we report the preservation of human RBC morphology, mechanics, and function following vitrification using a novel cryo-ink integrated with a cryo-printer, a droplet generation tool that can transform a bulk volume of human blood into nanoliter droplets on a cryo-paper. The results reveal that the recovered RBCs after ectoine-assisted vitrification, maintained their characteristic features, such as morphology, submembranous spectrin-actin network, and mechanical properties. In addition, the essential functions of recovered RBCs such as phosphorylation of band-3 protein, expression of complement receptor 1, and maintenance of intracellular nitric oxide and the reactive oxygen species are effectively preserved.

To transform a bulk sample of RBCs into nanoliter volume droplets in a bio-inspired cryo-ink, we developed a cryo-printing methodology (**Figure 1**). In this method, the cryo-ink acts as a cryoprotective agent to help the cells overcome the shock during the cooling and rewarming processes of cryopreservation. The cryo-printer contains an ejector in which the RBC-CPA mixture and the nitrogen gas are simultaneously expelled leading to the formation of nanoliter size droplets at the ejector outlet (Figure 1a). The cryo-printer in our experiments produces considerably small volumes of droplets (0.14 ± 0.096 nL, Figure S1 in the Supporting Information (SI)), with the aim being to minimize the adverse effects on RBCs by eliminating the requirements of high CPA concentrations to achieve vitrification. Vitrification using nanoliter droplets requires low concentrations of CPA (4.5%), while conventional methods, which utilize bulk volumes (450–500 mL), require high concentrations of CPAs (20–40%). Such high concentrations of CPAs loaded into bulk samples for conventional methods have been reported to cause adverse effects on RBCs.[14] In addition, small volumes of droplets provide ultra-high cooling and rewarming rates that enable preservation of cells without ice crystal formation.

Prior to cooling, blood samples were loaded with a cryo-protective ink at 1:1 dilution. A possible osmotic shock emerging from the exposure to the cryo-ink that could lead to RBC loss, was evaluated via hemolysis and revealed to be insignificant (Figure S2 in the SI). This cryo-ink contains ectoine (9% v/v), trehalose (25 μg mL^{-1}), and polyethylene glycol (PEG, 1% v/v) (Figure 1b). The optimal concentration of ectoine in the cryo-ink was determined as a result of a set of hemolysis analysis (Figure S3 in the SI). Ectoine is a naturally occurring solute present in the extremophilic bacteria which are capable of adapting to extreme thermal and osmotic stress conditions.[15] This capability is associated with the preferential exclusion of ectoine at the interface of a lipid monolayer of the cell membrane. The exclusion leads to expansion of the membrane, promoting the penetration of water molecules.[16,17] The increased number of water molecules in the vicinity of the lipids improves the membrane fluidity, which is crucial to withstand osmotic shock and to assist in the cell repair mechanisms.[16] Ectoine-containing CPA solutions have previously been employed for mesenchymal stem-cell preservation with conventional slow-freezing protocols.[11] The cryo-ink solution used in this study contains in addition to ectoine, trehalose, and PEG, which have complementary enhancing effects.[18,19] For example, PEG suppresses the freezing point of the solution.[19] We utilized vitrification (below –150 °C) as a cooling method instead of conventional freezing (–80 °C or above) to minimize cryo-injury.[52] Vitrification occurs when the CPA-loaded RBCs are super-cooled down to the glass-transition temperature and adopt a glass-like amorphous morphology.[10] This is different than conventional freezing where the cell injury, caused by the formation of ice crystals, is of concern.[10,20] The printing of the nanoliter droplets on a cryo-paper (nonporous polyethylene collection film with 8.5 cm in diameter) and subsequent submersion into liquid nitrogen (–196 °C) results in immediate vitrification of the RBCs (Figure 1c). One of the major challenges in conventional vitrification is ice crystallization, which occurs during rapid rewarming.[10] Ice crystallization occurs as a result of the latent heat of fusion, causing hemolysis of the cells.[10] To avoid such crystallization, vitrified blood sample was ultra-rapidly rewarmed by immersing the printed nanoliter droplets on cryo-paper in warm media (≥37 °C) (Figure 1b). Furthermore, utilizing bio-inspired CPAs; such as ectoine and trehalose, in low concentrations eliminates extensive washing steps that are required for other protocols, such as glycerol-based techniques. The washing step is minimal in this method and is achieved by re-suspending the RBCs in PBS.

The extent of cryo-injury on RBCs is reflected by their altered morphology. Healthy RBCs have a unique biconcave-discoid morphology (**Figure 2**a, i, m, and S5, S6, and S7 in the SI).

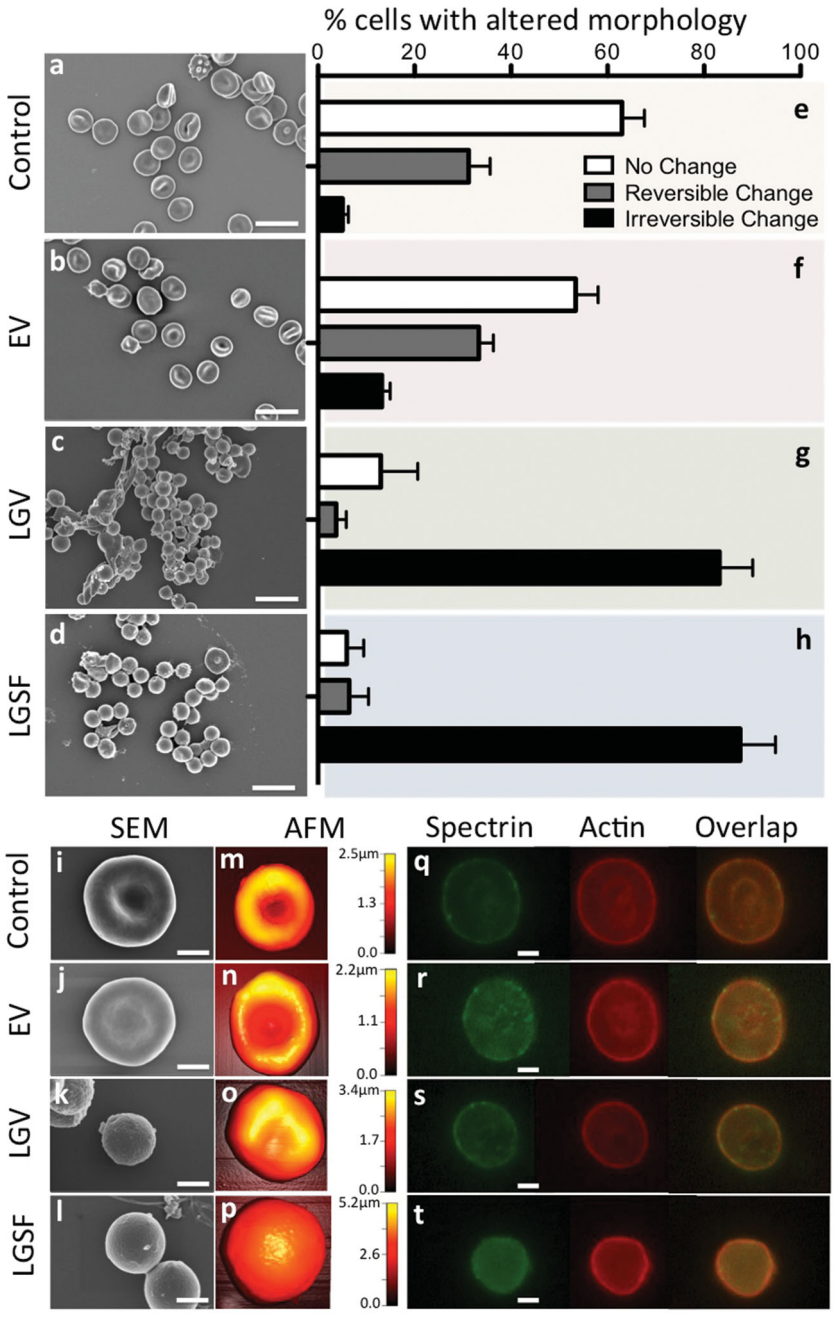

Figure 2. Assessment of RBC morphology following ectoine-based vitrification and rewarming. a–d) Scanning electron micrographs of RBCs: a) selected directly from blood, and recovered after: b) ectoine-based vitrification (EV), c) low-glycerol vitrification (LGV), and, d) low-glycerol slow freezing (LGSF). e–h) The percentage (%) of RBCs within a population representing: e) untreated fresh blood, and blood recovered from: f) EV, g) LGV, and, h) LGSF: biconcave shape, and reversible and irreversible shape changes (*n*, number of cells = 114–309, and *N*, number of donors = 3–9). Error bars in figures represent the standard error of the mean. i–l) Higher magnification (30 000×) of SEMs of: i) fresh RBCs, and RBCs recovered after: j) EV, k) LGV, and, l) LGSF. m–p) Atomic force micrographs of: m) fresh RBCs, and RBCs recovered after: n) EV, o) LGV, and, p) LGSF. q–t) Fluorescence micrographs showing distribution of the spectrin-actin network in RBCs. q) RBCs in fresh blood, and RBCs recovered from: r) EV, s) LGV, and t) LGSF. Scale bar represents 10 μm in a–d and 2 μm in i–l and q–t.

The biconcave shape increases the oxygen-delivering capacity of RBCs provided by the high surface area in close proximity to the vessel walls.[21] Additionally, RBCs owe their extreme flexibility to their biconcave shape,[22] which allows them to travel through the microvasculature. If RBCs are challenged by mild environmental fluxes such as slight osmotic changes,[23] reversible morphological alterations may occur. One example is the transformation to echinocytes (Figure S4 in the SI), where the plasma membrane exhibits small projections.[24] Irreversible shape changes of RBCs are indicated by the formation of spherocytes, the completely round forms of RBCs.[25] To investigate the changes in morphology of recovered RBCs subsequent to ectoine-based vitrification (EV), a series of scanning electron micrographs (SEMs) were obtained (Figure 2a–d and S5a–r in the SI). The cells visualized by SEM were categorized under three different groups exhibiting: i) no change (biconcave discocytes), ii) reversible change (e.g., echinocytes and stomatocytes), and, iii) irreversible change (spherocytes).[26] For each group, the number of recovered cells was considered to be the total count of the biconcave RBCs and the RBCs that exhibit reversible changes. Approximately 94% of the RBCs in the fresh blood sample have the characteristic RBC morphology (Figure 2e). Likewise, approximately 88% of RBCs during the EV maintained their original form (Figure 2f). We compared these results to alternative cryopreservation methods including low-glycerol vitrification (LGV) and low-glycerol slow freezing (LGSF). The RBCs recovered after LGV and LGSF go through significant irreversible shape changes (mainly spherocytes): 83% and 88% of the entire population of cells, respectively (Figure 2g and h). This is in agreement with the previous observations of the transformation of biconcave human RBCs[4] and mesenchymal stem cells[11] to spherocytes upon glycerol-based cryopreservation. Figure 2i–l include high-magnification SEMs of the recovered RBCs. SEMs of RBCs with various magnifications during each step in cryopreservation protocols are also shown in Figure S5. To evaluate the topographical maps of recovered RBCs, we performed atomic force microscopy (AFM; Figure 2m–p). The results are in agreement with the SEM observations and confirm the biconcave shape of cells in the control group and of the recovered cells after EV. The maps show cells that experienced LGV and LGSF became spherocytes. Spherocytes are undesired forms of RBCs and such irreversible shape changes of RBCs are related to decreased function and diseases: studies investigating the impact of irreversibly

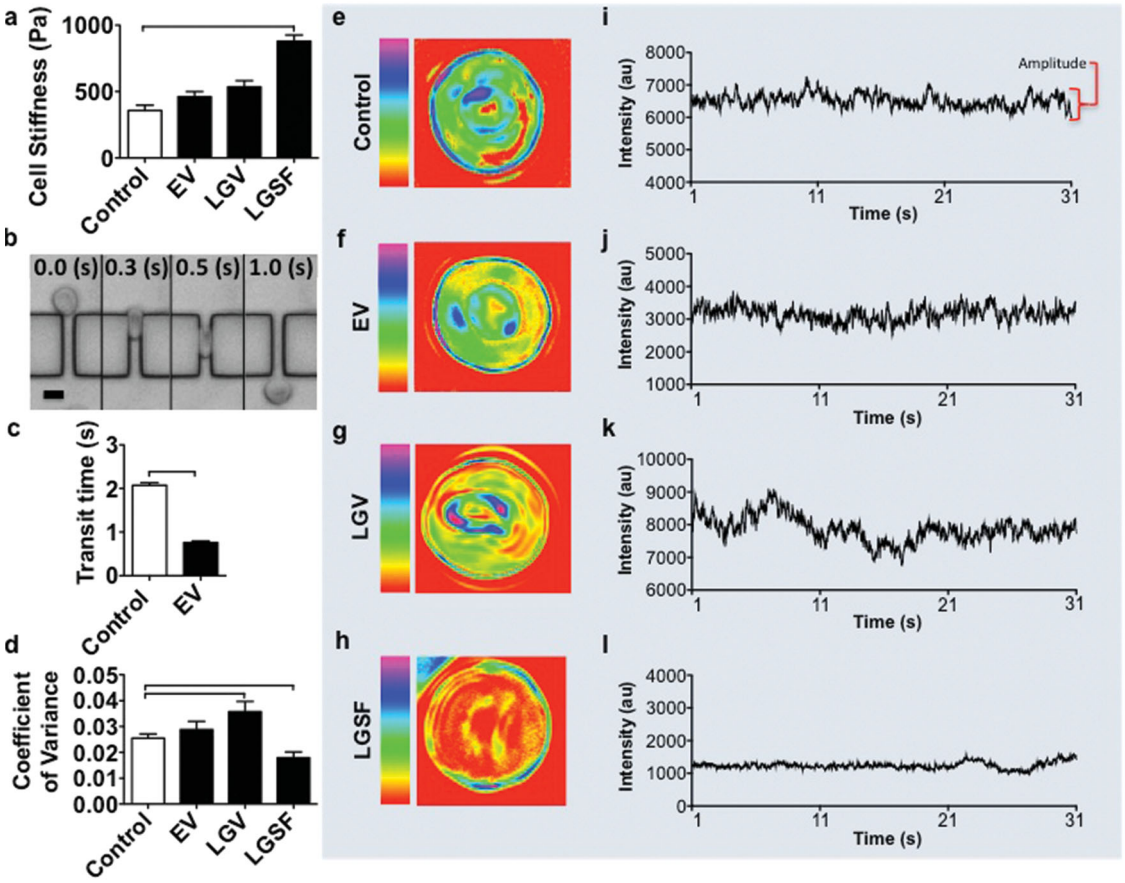

Figure 3. Assessment of RBC biomechanics following ectoine-based vitrification and rewarming. a) Cell stiffness determined via AFM for fresh RBCs as well as for RBCs recovered after EV, LGV, and LGSF. The measurements were performed on recovered RBCs following plasma re-suspension (n = 30–45 and N = 3). b) Light microscopy time-series of a recovered RBC (after EV) passing through the microchannel array. The scale bar represents 4 µm. RBC deformability was measured as the time required for the cell to go through and exit the channel (height = 2 µm and width = 4.5 µm). c) Deformability determined for fresh RBCs (n = 192) and for RBCs recovered after EV (n = 245), N = 3. d–l) Cell membrane flickering: d) Membrane flickering as a function of coefficient of variance determined for fresh RBCs and RBCs recovered after EV, LGV, and LGSF, (n = 14–40, N = 1–3); e–h) detailed flickering profiles of individual RBCs; pseudo-color images represent a heat map of the coefficient of variance of: e) fresh RBC, and recovered RBCs after: f) EV, g) LGV, and, h) LGSF. The red color represents the minimum intensity coefficient of variance (flickering) while the magenta color represents the maximum coefficient of variance. i–l) Time series of coefficient of variance of a single representative pixel from heat maps of: i) fresh RBCs, and recovered RBCs after: j) EV, k) LGV, and l) LGSF. The intensity is represented in arbitrary units (au). Error bars in the figures represent the standard error of the mean. Connecting brackets between the individual groups indicate statistically significant results ($p < 0.05$).

altered RBC morphology after transfusion of stored blood have reported a reduced capacity of RBCs to oxygenate the tissues,[27] increasing the risk for peripheral ischemia and deep venous thrombosis.[28] Spectrin and actin proteins construct the major backbone of the RBC skeleton, which is altered when these proteins are damaged.[22] To investigate the effect of EV on the RBC cytoskeleton, we performed immunocytochemistry to evaluate the distribution of spectrin (α- and β-chains) and actin filaments of recovered cells (Figure 2q–t). The pattern distribution across the recovered RBCs after EV was comparable to the control RBCs (Figure 2q and r). The RBCs recovered after LGV and LGSF showed different protein distribution patterns where the central spectrin-actin region was distorted (Figure 2s) or disintegrated (Figure 2t and S6 in the SI).

To test the mechanical properties of recovered RBCs, we evaluated the membrane stiffness, cell deformability, and membrane flickering. Cell stiffness was evaluated by measuring the elastic moduli of the cells using AFM.[54] The stiffer the cell, the higher its elastic modulus.[29] Recovered RBCs after EV displayed comparable stiffness (461 ± 38 Pa) to control RBCs (358 ± 38 Pa; **Figure 3**a). The recovered cells were incubated in autologous plasma for 3 h to evaluate the membrane stiffness ex vivo. On the other hand, RBCs recovered after LGSF displayed greater ($p < 0.05$) stiffness (879 ± 47 Pa, Figure 3a) compared to the control. Another characteristic of RBCs is their significant deformability which enables them to pass through capillary veins and exchange oxygen and carbon dioxide with cells in tissues.[30] We have measured the deformability by forcing the recovered RBCs to pass through 4.5 µm wide and 2 µm high microchannels (Figure 3b) and by evaluating the duration of their travel along the channels (Figure 3c). This evaluation is based on the findings from previous reports[31] which indicate a relatively more flexible cell would be able to pass through the channel in a shorter time, compared with a less-deformable cell.

The RBCs recovered from EV passed through the microfluidic channels 1.3 s faster on average compared with control RBCs (Figure 3c). The difference is statistically significant ($p < 0.05$) and indicates higher deformability of the recovered cells after EV. The measurements were performed on the fresh blood at room temperature (20–24 °C). The corresponding measurements on recovered RBCs from EV were also performed at room temperature but after the cells experienced significant temperature changes during cooling and rewarming (–198 to 37 °C). The increase in the deformability of RBCs measured in a similar microfluidic system was linked to temperature changes.[32] An increase in RBC deformability was previously investigated but was not linked to negative effects[5,33] whereas a decrease in deformability was associated with blood related diseases[30,34] and low quality of stored blood.[2] The analysis on the deformability of the RBCs could not be performed for the LGV and LGSF due to blockage of microchannels by the RBCs in these two groups. Earlier reports have associated the reduced deformability in stored RBCs with irreversible shape changes, such as those observed for spherocytes.[35]

The membrane flickering of recovered cells, also known as fluctuations or oscillations, was evaluated as a functional response of RBCs.[36] The flickering was quantified by recording changes in light scattering at the surface of a RBC using time-lapse, positive-low phase-contrast microscopy over a period of 30 s at frequency of 33 frames s^{-1} (Figure 3d–l). The intensity of scattered light was used to calculate the coefficient of variance at each point. These fluctuations show that the recovered RBCs after EV maintained their flickering amplitude at levels comparable with fresh RBCs (Figure 3d). However, the amplitude of membrane flickering in the recovered cells after LGV and LGSF differs significantly ($p < 0.05$) from both control and recovered RBCs after EV (Figure 3d). Loss of flickering amplitude has been observed in RBCs during multiple diseases, such as systemic lupus erythematosus and malaria infection.[30,37] The pseudo-color images in Figure 3e–h represent a map of the coefficient of variance on the RBCs measured as a sum of each pixel covering the cell surface during 30 s. Figure 3i–l shows the amplitude of intensity of a representative pixel corresponding to the pseudo-color images in Figure 3e–h.

To evaluate the functional properties of EV recovered RBCs, we measured band-3 phosphorylation (**Figure 4**a), CD35 expression (Figure 4b), intracellular nitric oxide (NO) (Figure 4c), and intracellular reactive oxygen species (ROS) (Figure 4d). The measurements were performed by flow cytometry after incubation in 25% serum from a known universal donor. Band-3 is an integral protein that regulates RBC membrane organization and function.[38] Alteration of band-3 phosphorylation levels has been associated with increased rigidity of RBCs, therefore, decreasing their perfusion to host organs and their lifespan in the circulation.[39] Although there was a slight decrease of band-3 phosphorylation level in recovered RBCs after EV (geometric mean: 25) compared to control RBCs (geometric mean: 29.7), the decrease was not significant (Figure 4a). CD35 (also known as complement receptor 1, CR1), is a unique human RBC regulatory protein,[40] critical in the immune-clearance process and thus for the maintenance of a non-inflammatory intravascular environment.[41] Injury associated with RBC storage changes the tendency of CD35 to cluster on the cell membrane, which ultimately reduces the ability of the cell to capture and transport the inflammatory particles, thereby maintaining the non-inflammatory status of the circulatory system.[41] The recovered RBCs after EV showed a comparable CD35 expression level to the control RBCs that were collected from the same donor with geometric means of 7.5 and 8.0, respectively (Figure 4b).

The intracellular NO and ROS levels as regulators for blood flow and RBC homeostasis were also evaluated.[42] NO is a crucial short-lived signaling molecule regulating local vasodilation.[43] Loss of NO has been observed after prolonged storage of RBCs and it has been linked to biochemical (e.g., depletion of adenosine triphosphate and 2,3-diphosphoglycerate) or hemolysis-related changes including morphology and deformability changes.[44] Formation of ROS during the preservation process has been also shown to accelerate RBC storage injury and significantly reduce post-transfusion RBC viability.[45] ROS are highly reactive molecules that target a wide range of cell components, including lipids, nucleic acids, and proteins (i.e., spectrin in RBCs), which undergo irreversible ROS-mediated changes resulting in significant decreases in RBC deformability.[46] Our results demonstrated that the cells recovered after EV maintained the intracellular NO (geometric mean: 9.6) and ROS levels (geometric mean: 6.7) compared to control RBCs (geometric means: 8.8 and 7.2, respectively) (Figure 4b–d). In addition, flow cytometry results clearly reveal the preservation of recovered RBC morphology after EV, fully supporting our SEM and AFM results shown in Figure 1 (see Figure S7 in the SI).

In this study, we report the preservation of human red blood cell (RBC) morphology, mechanics, and function following vitrification in nanoliter volumes using an innovative cryo-ink integrated with a bio-printing approach. The use of nano-liter droplet vitrification for the purpose of cryopreservation of RBCs has not been well studied or applied,[10] although it could potentially provide a powerful means to cryopreserve RBCs for blood banking. One challenge is the transformation of the concept into a high-throughput system where large volumes of blood are rapidly vitrified. We have previously demonstrated the scalability of droplet system by developing arrays consisting of multiple ejectors for droplet generation, which could potentially enables automation and high-throughput processing.[47] We envision that a series of such arrays would provide rapid printing of droplets for bulk volumes of blood samples before vitrification. Furthermore, the presented method has the potential to minimize cell contamination by using sterilized liquid nitrogen (LN_2). It has been shown that LN_2 can be sterilized by utilizing ultraviolet radiation,[48] or sterile PTFE cartridge filters,[49] minimizing such contamination risks.[50] Therefore, the presented method has the potential for minimizing such contamination risks and allowing the sterilization of potential automated high-throughput applications by bringing multiple ejectors together. Additionally, we observed a mild increase in the hemolysis when using the polyethylene collection film (Figure S8 in the SI). The hemolysis at this collection step could be eliminated with the use of materials that would enable less mechanical stress upon collection, for example a soft and biocompatible fibrin film. The RBCs cryoprinting step was also evaluated and compared with manually pipetting of CPA-loaded RBCs (control). None of the printed groups (EV and LGV) show significant increase in hemolysis

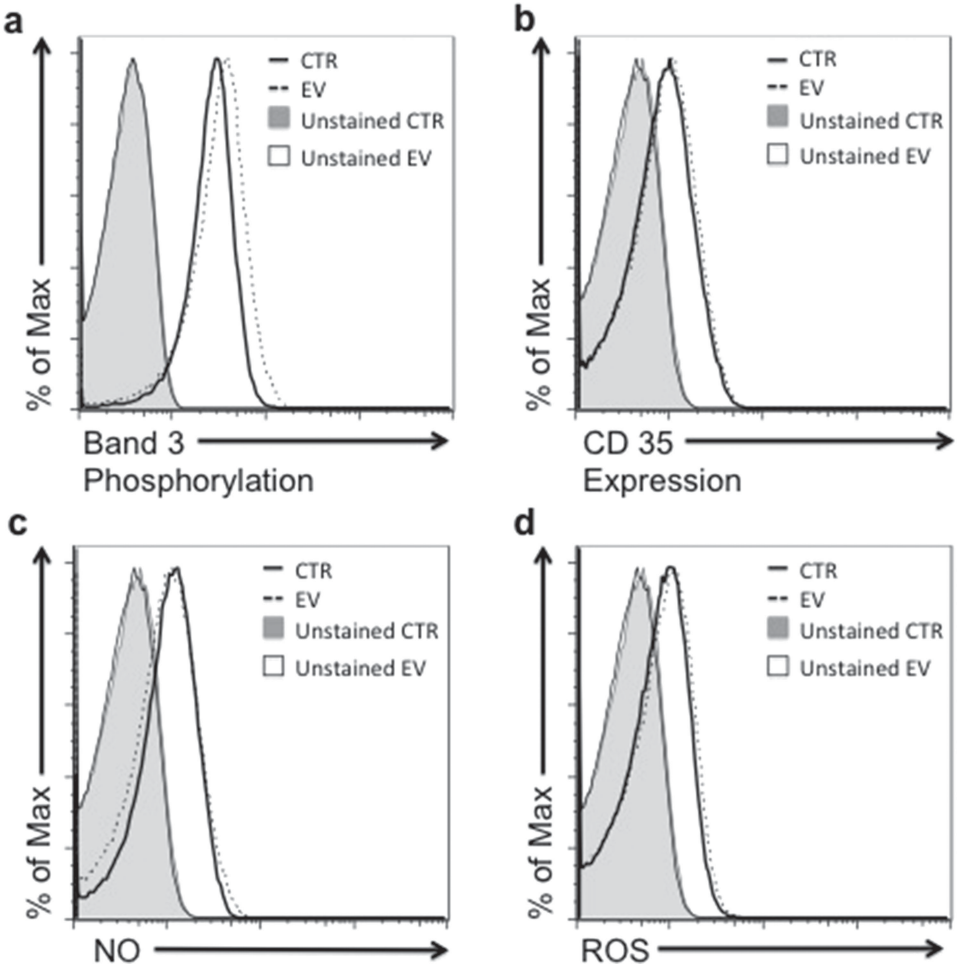

Figure 4. Assessment of RBC functional properties following ectoine-based vitrification and rewarming. a–d) Functional properties for fresh RBCs (control, solid line) and recovered RBCs after ectoine-based vitrification (EV, dotted line) were compared. Four types of characteristic RBC function were measured: a) determined band-3 phosphorylation level, b) CD35 expression, c) intracellular nitric oxide (NO) level, and, d) intracellular reactive oxygen species (ROS) level. The negative controls (unstained fresh RBCs represented by the gray shaded region and unstained recovered RBCs after EV represented by the dashed line) were not labeled and were used as a baseline to detect the auto-fluorescence of cells. The measurements were performed following incubation of RBCs with 25% serum from a universal donor for 30 min at 37 °C.

above the acceptable level, thereby validating the cryoprinting-based system (Figure S8 in the SI).

Here, we demonstrated the cryo-printing of the ectoine-loaded RBCs encapsulated in nanoliter droplets. The printed RBCs on cryo-paper were vitrified in extremely low temperatures. After rewarming the maintenance of RBC morphology, mechanics, and function were evaluated. Ectoine-assisted cryo-printing has the potential to improve the efficiency of blood banking and further create new approaches to biopreserve various cell types, including stem cells, natural killer cells, and gametes.

Conflict-of-Interest Statement

Dr. U. Demirci is a founder of, and has an equity interest in: (i) DxNow Inc., a company that is developing microfluidic and imaging technologies for point-of-care diagnostic solutions, and (ii) Koek Biotech, a company that is developing microfluidic IVF technologies for clinical solutions. Dr. U. Demirci's interests were viewed and managed by the Brigham and Women's Hospital and Partners HealthCare in accordance with their conflict-of-interest policies. Dr. U. Demirci is a scientific advisory board member of Akron Biotechnology. Dr. C. Zylberberg is the Chief Executive Officer of Akron Biotechnology. Akron Biotechnology provided the ectoine solution.

Supporting Information

Supporting Information is available from the Wiley Online Library or from the author.

Acknowledgements

This work was performed at the Bio-Acoustic MEMS in Medicine (BAMM) Labs at the HST-BWH, Harvard Medical School. The authors would like to acknowledge their appreciation to the late Dr. Aida Nureddin for her

significant contributions to this project. She was instrumental in the design, execution, and interpretation of this data. Dr. Nureddin's intellect and pleasant demeanor will be sorely missed. We would like also to thank April Holland, Maria Lebruto, Mark Melhon, Burcu Erkmen, Vasily Giannakeas, Josh Samot, Waseem Asghar, Zhang Xu, Fatih Inci, Andrea Pena, Sandra Boehler, Muntasir Jahangir, and Remington Willenbrecht for technical support and discussion throughout the research project. We would like to thank Quang Le, Daniel Martinenz, and Hassan Sakhta for contributing in this study as high school students under the Student Success Job Program at Brigham and Women's Hospital, Harvard Medical School and under Dr. Demirci's NSF Career Award # 1150733. We would also like to thank Mudit Tandon from Belmont Hill School and Srikar Srivatsa from Cupertino High School for contributing to this study. Following this study Quang Lee, Daniel Martinenz, Mudit Tandon, and Hassan Sakhta joined the University of Massachusetts, Harvard University, Tuft University, and Northeastern University, respectively, for their college education. This work was partially supported by NIH R21-HL095960, NIH R01-EB015776, NIH R01-HL096795, and NIH U54EB15408. Irep Gozen was supported by the Swedish Research Council-Vetenskapsrådet. *Author Contributions*: R.E. and U.D. developed the idea; R.E., S.G., U.A.G., N.L., R.K., Q.W., I.G., and U.D. designed the experimental approach; R.E., S.G., U.A.G., H.S., S.D., N.A., GT, JE, JK, Q.W., W.F., G.T., Q.W., and I.G. performed the experiments; R.E., S.G., U.A.G., I.G., G.T., B.I., R.K., C.Z., N.L., Q.W., I.G., and U.D. analyzed the data; RE, SG, UAG, IG, SD, NA, W.F., Q.W., I.G., and U.D. wrote the manuscript.
Note: The acknowledgements were updated on September 1, 2014.

Received: February 28, 2014
Revised: May 12, 2014
Published online: July 22, 2014

[1] a) D. Discher, N. Mohandas, E. Evans, *Science* **1994**, *266*, 1032; b) N. Mohandas, J. Chasis, *Seminars in Hematology* **1993**.
[2] E. Bennett-Guerrero, T. H. Veldman, A. Doctor, M. J. Telen, T. L. Ortel, T. S. Reid, M. A. Mulherin, H. Zhu, R. D. Buck, R. M. Califf, T. J. McMahon, *Proc. Natl. Acad. Sci. USA* **2007**, *104*, 17063.
[3] C. G. Koch, L. Li, D. I. Sessler, P. Figueroa, G. A. Hoeltge, T. Mihaljevic, E. H. Blackstone, *New Engl. J. Med.* **2008**, *358*, 1229.
[4] V. Pallotta, G. M. D'Amici, A. D'Alessandro, R. Rossetti, L. Zolla, *Blood Cells Mol. Diseases* **2012**, *48*, 226.
[5] S. Henkelman, J. W. Lagerberg, R. Graaff, G. Rakhorst, W. Van Oeveren, *Transfusion* **2010**, *50*, 2393.
[6] J. L. Holovati, K. A. Wong, J. M. Webster, J. P. Acker, *Transfusion* **2008**, *48*, 1658.
[7] H. T. Meryman, M. Hornblower, *Transfusion* **1972**, *12*, 145.
[8] A. W. Rowe, E. Eyster, A. Kellner, *Cryobiology* **1968**, *5*, 119.
[9] K. L. Scott, J. Lecak, J. P. Acker, *Transfusion Med. Rev.* **2005**, *19*, 127.
[10] H. T. Meryman, *Transfusion* **2007**, *47*, 935.
[11] T. A. Grein, D. Freimark, C. Weber, K. Hudel, C. Wallrapp, P. Czermak, *Int. J. Artificial Organs* **2010**, *33*, 370.
[12] a) U. A. Gurkan, R. El Assal, S. E. Yildiz, Y. Sung, A. J. Trachtenberg, W. P. Kuo, U. Demirci, *Mol. Pharm.* **2014**; b) E. Ceyhan, F. Xu, U. A. Gurkan, A. E. Emre, E. S. Turali, R. El Assal, A. Acikgenc, C.-a. M. Wu, U. Demirci, *Lab Chip* **2012**, *12*, 4884; c) U. Gurkan, Y. Sung, R. El Assal, F. Xu, A. Trachtenberg, W. Kuo, U. Demirci, *J Tissue Eng Regen Med* **2012**.
[13] N. G. Durmus, S. Tasoglu, U. Demirci, *Nat. Mater.* **2013**, *12*, 478.
[14] D. Mantzavinos, A. Bailey, M. Rampling, *Biorheology* **1997**, *34*, 73.
[15] K. Lippert, E. A. Galinski, *Appl. Microbiol. Biotechnol.* **1992**, *37*, 61.
[16] R. K. Harishchandra, S. Wulff, G. Lentzen, T. Neuhaus, H. J. Galla, *Biophys. Chem.* **2010**, *150*, 37.
[17] J. M. Pastor, M. Salvador, M. Argandoña, V. Bernal, M. Reina-Bueno, L. N. Csonka, J. L. Iborra, C. Vargas, J. J. Nieto, M. Cánovas, *Biotechnol. Adv.* **2010**, *28*, 782.
[18] I. S. Bhandal, R. M. Hauptmann, J. M. Widholm, *Plant Physiol.* **1985**, *78*, 430.
[19] S. Ohboshi, N. Fujihara, T. Yoshida, H. Tomogane, *Anim. Reprod. Sci.* **1997**, *48*, 27.
[20] a) D. E. Pegg, in *Cryopreservation and Freeze-Drying Protocols*, Springer **2007**, *39*; b) J. O. Karlsson, M. Toner, *Biomaterials* **1996**, *17*, 243.
[21] M. M. Guest, T. P. Bond, R. G. Cooper, J. R. Derrick, *Science* **1963**, *142*, 1319.
[22] N. Mohandas, P. G. Gallagher, *Blood* **2008**, *112*, 3939.
[23] C. Mrowietz, B. Hiebl, R. Franke, J.-W. Park, F. Jung, *Clinical Hemorheol. Microcirculation* **2008**, *39*, 281.
[24] M. Stasiuk, G. Kijanka, A. Kozubek, *Postepy Biochem.* **2009**, *55*, 425.
[25] J. C. Cluitmans, M. R. Hardeman, S. Dinkla, R. Brock, G. J. Bosman, *Blood Transfusion (Trasfusione del Sangue)* **2012**, *10* (Suppl. 2), s12
[26] a) M. Bessis, *Nouvelle Revue Francaise d'Hematologie* **1972**, *12*, 721; b) J. Laczko, C. Feo, W. Phillips, *Transfusion* **1979**, *19*, 379.
[27] a) A. Tinmouth, D. Fergusson, I. C. Yee, P. C. Hébert, *Transfusion* **2006**, *46*, 2014; b) G. Bosman, J. Werre, F. Willekens, V. Novotný, *Transfusion Med.* **2008**, *18*, 335.
[28] a) E. Alt, S. Banyai, M. Banyai, R. Koppensteiner, *Thrombosis Res.* **2002**, *107*, 101; b) S. Yedgar, A. Koshkaryev, G. Barshtein, *Pathophysiol. Haemostasis Thrombosis* **2003**, *32*, 263.
[29] V. K. Katiyar, D. Fisseha, *World* **2011**, *1*, 100.
[30] I. C. Ghiran, M. L. Zeidel, S. S. Shevkoplyas, J. M. Burns, G. C. Tsokos, V. C. Kyttaris, *Arthritis Rheumatism* **2011**, *63*, 503.
[31] A. Adamo, A. Sharei, L. Adamo, B. Lee, S. Mao, K. F. Jensen, *Anal. Chem.* **2012**, *84*, 6438.
[32] S. Huang, H. Bow, M. Diez-Silva, J. Han, Massachusetts Institute of Technology **2011**. http://hdl.handle.net/1721.1/66032
[33] H. Mairbäurl, *Frontiers Physiol.* **2013**, *4*, DOI:10.3389/fphys.2013.00332.
[34] S. M. Hosseini, J. J. Feng, *Biophys. J.* **2012**, *103*, 1.
[35] a) G. M. Wagner, D. T. Chiu, J. H. Qju, R. H. Heath, B. H. Lubin, *Blood* **1987**, *69*, 1777; b) R. Card, N. Mohandas, P. Mollison, *Br. J. Haematol.* **1983**, *53*, 237.
[36] M. Costa, I. Ghiran, C.-K. Peng, A. Nicholson-Weller, A. L. Goldberger, *Phys. Rev. E* **2008**, *78*, 020901.
[37] R. Chandramohanadas, Y. Park, L. Lui, A. Li, D. Quinn, K. Liew, M. Diez-Silva, Y. Sung, M. Dao, C. T. Lim, *PloS ONE* **2011**, *6*, e20869.
[38] N. Mohandas, P. G. Gallagher, *Blood* **2008**, *112*, 3939.
[39] J. R. H. A. B. Zimrin, *Vox Sanguinis* **2009**, *96*, 93.
[40] J. Li, J. P. Wang, I. Ghiran, A. Cerny, A. J. Szalai, D. E. Briles, R. W. Finberg, *Infection Immunity* **2010**, *78*, 3129.
[41] C. H. Chen, I. Ghiran, F. Beurskens, G. Weaver, J. Vincent, A. Nicholson-Weller, L. Klickstein, *Clin. Exp. Immunol.* **2007**, *148*, 546.
[42] a) L. Gliemann, M. Nyberg, Y. Hellsten, *Free Radical Res.* **2013**, *1*; b) L. Kuo, N. Thengchaisri, T. W. Hein, *Mol. Med. Therap.* **2012**, *1*.
[43] M. Grau, S. Pauly, J. Ali, K. Walpurgis, M. Thevis, W. Bloch, F. Suhr, *PloS ONE* **2013**, *8*, e56759.
[44] J. Bonaventura, *Proc. Natl. Acad. Sci. USA* **2007**, *104*, 19165.
[45] a) I. Chin-Yee, N. Arya, M. S. d'Almeida, *Transfusion Sci.* **1997**, *18*, 447; b) T. Yoshida, J. AuBuchon, L. Tryzelaar, K. Foster, M. Bitensky, *Vox Sanguinis* **2007**, *92*, 22.
[46] A. G. Kriebardis, M. H. Antonelou, K. E. Stamoulis, E. Economou-Petersen, L. H. Margaritis, I. S. Papassideri, *J Cell. Mol. Med.* **2007**, *11*, 148.
[47] J. Samot, S. Moon, L. Shao, X. Zhang, F. Xu, Y. Song, H. O. Keles, L. Matloff, J. Markel, U. Demirci, *PloS ONE* **2011**, *6*, e17530.

[48] L. Parmegiani, G. E. Cognigni, M. Filicori, *Hum. Reprod.* **2009**, *24*, 2969.
[49] L. D. McBurnie, B. Bardo, *Pharm. Technol. N. Am.* **2002**, *26*, 9.
[50] A. Bielanski, G. Vajta, *Hum. Reprod.* **2009**, *24*, 2457.
[51] S. Tasoglu, U. A. Gurkan, S. Wang, U. Demirci, *Chem. Soc. Rev.* **2013**, *42*(13), 5788–808.
[52] Y. S. Song, D. Adler, F. Xu, E. Kayaalp, A. Nureddin, R. M. Anchan, R. L. Maas, U. Demirci, *Proc. Natl. Acad. Sci. USA* **2010**, *107*, 4596–600.
[53] W. Asghar, R. El Assal, H. Shafiee, R. M. Anchan, U. Demirci, *Biotechnol. J.* **2014**, *9*, DOI:10.1002/biot.201300074.
[54] G. Thomas, N. A. Burnham, T. A. Camesano, Q. Wen, *J. Vis. Exp.* **2013**, Issue 76.